Journal of Power Sources 196 (2011) 7594–7600

Contents lists available at ScienceDirect

Journal of Power Sources

journal homepage: www.elsevier.com/locate/jpowsour

Electrochemical and fuel cell evaluation of Co based catalyst for oxygen reduction in anion exchange polymer membrane fuel cells

M. Mamlouk[a,*], S.M. Senthil Kumar[a], Pascal Gouerec[b], Keith Scott[a]

[a] School of Chemical Engineering and Advanced Materials, Merz Court, University of Newcastle, Newcastle upon Tyne NE1 7RU, United Kingdom
[b] GPMaterials, Le Mirabeau, 11 bd Chantemerle, Aix les Bains 73100, France

ARTICLE INFO

Article history:
Received 2 February 2011
Received in revised form 19 April 2011
Accepted 20 April 2011
Available online 28 April 2011

Keywords:
Alkaline membrane fuel cell
Anion exchange
Cobalt
Oxygen reduction
Non precious metal catalysts

ABSTRACT

Co based catalyst were evaluated for oxygen reduction (ORR) in liquid KOH and alkaline anion exchange membrane fuel cells (AAEMFCs). In liquid KOH solution the catalyst exhibited good performance with an onset potential 120 mV more negative than platinum and a Tafel slope of ca. 120 mV dec^{-1}. The hydrogen peroxide generated, increased from 5 to 50% as the electrode potential decreased from 175 to −300 mV vs. SHE.

In an AAEMFC environment, one catalyst (GP2) showed promising performance for ORR, i.e. at 50 mA cm^{-2} the differences in cell potential between the stable performance for platinum (more positive) and cobalt cathodes with air and oxygen, were only 45 and 67 mV respectively. The second catalyst (GP4) achieved the same stable power density as with platinum, of 200 and 145 mW cm^{-2}, with air at 1 bar (gauge) pressure and air (atm) cathode feed (60 °C), respectively. However the efficiency was lower (i.e. cell voltage was lower) i.e. 40% in comparison to platinum 47.5%.

1. Introduction

Solid (cation-free) OH^- ion conducting polymer alkaline electrolyte membranes (AEM) could hold the key answer to many of the limitations of polymer electrolyte membrane fuel cell (PEMFC). AEMs exhibit several advantages over PEMFCs including: the oxygen reduction reaction (ORR) is faster under alkaline conditions than in acidic conditions therefore providing lower activation losses [1], non-precious metal catalysts (NPMCs) can be used quite effectively [2], increased number of cheap materials for cell components due to less corrosive environment [3]. Other major issues with PEMFCs of water management, cross-over and cathode flooding are potentially addressed in AEMFCs by water and ion transport away from the cathode to the anode mitigating crossover and flooding problems [4].

AEMs are solid polymer electrolyte membranes that contain positive ionic groups (e.g., quaternary ammonium (QA) functional groups such as poly–N^+CH_3) and mobile negatively charged anions (e.g., usually OH^-). Several types of anion exchange membranes based on quaternary ammonium groups were reported in the literature, radiation-grafted PVDF, ETFT, and FEP polymers containing vinylbenzyl chloride (VBC) units [5–7], quaternized poly(ether sulfone) PES [8–10], quaternized poly(2,6-dimethyl-1,4-phenylene oxide) PPO [11], quaternized poly(phthalazinone ether sulfone ketone) PPESK [12], quaternized poly(phenylene) [13,14] and quaternized copolymer of poly(methyl methacrylate-co-butyl acrylate-co-vinylbenzyl chloride) [15].

There are several well-known chemistries and classes of non-precious cobalt catalyst materials for the oxygen reduction reaction (ORR) in alkaline media including: Co phthalocyanines (CoPc) [16], cobalt fullerene complexes [17], cobalt–iron–nitrogen chelate Co–C–N [18,19], cobalt-hexadecafluoro-phthalocyanine (CoPcF16) [20], polypyrrole-modified carbon-supported $Co(OH)_2$-PPY-C/GC [21], Co containing precursor and a polypyrrole/C composite material (PPy/C) [22] and other cobalt macrocycles [23].

Most of the Co containing precursors and a polypyrrole/C composite material, exhibit a dual site functionality [22] where O_2 initially is reduced at a Co^{2+} containing N–C type site in a 2e$^-$ process to form H_2O_2, which can react further in the series type ORR mechanism at the decorated Co_xO_y/Co nano-particle surface undergoing either further electrochemical reduction to form OH^- species or chemical disprotonation to form OH^- species and molecular O_2 [22].

Rotating disk electrode (RDE) and rotating ring disk electrode (RRDE) measurements have also showed that the ORR mechanism is via a 2e$^-$ pathway on most of the reported Co based catalyst in the literature with a Tafel slope of 120 mV dec^{-1}. Values for the number of electrons (n) in the ORR at the higher potential region ($E < -100$ mV vs. Hg/HgO) are reported to be ca. 2 for CoPc/C catalyst [20,24], in a range of 1.4–2.4 for CoPc/C [24,25], an apparent 2e$^-$ for CoPcF16 [20] and values between 2.4 and 3 for CoTAA [26]. Similarly, cobalt (II) porphyrins, $TpOCH_3PPCo$, $TpCF_3PPCo$ and TpF-

* Corresponding author. Tel.: +44 191 222 5207; fax: +44 191 222 5292.
E-mail address: mohamed.mamlouk@ncl.ac.uk (M. Mamlouk).

0378-7753/$ – see front matter © 2011 Elsevier B.V. All rights reserved.
doi:10.1016/j.jpowsour.2011.04.045

PPCo exhibited apparent values of n of 3, 2 and 2, respectively [23] and the polypyrrole-modified carbon-supported $Co(OH)_2$-PPY-C/GC exhibited n number between the 2 and 4 electron reduction of O_2 [21].

The dominant $2e^-$ process for ORR on Co containing precursors to form H_2O_2 is also demonstrated by high amount of H_2O_2 produced The percentage of H_2O_2 detected from RRDE measurements was between 30 and 70% in the potential range of 0.70 and 0.10 V (vs. RHE) for Co–C–N [18], 50 and 5% for Co-TMPP pyrolysed at 400 and 800 °C, respectively [27], and 40–50% for the pyrolysed Co containing precursor and a polypyrrole/C composite material (PPy/C) [22].

There are many publications in the literature on the preparation and evaluation of Co based catalyst in three electrode cells, however, there is a limited data on its evaluation in an alkaline fuel cell environment and especially in an anion exchange membrane (AEM) fuel cells. Co-TMPP electrodes (176 mg cm^{-2}) were tested in liquid 5 M KOH at 40 °C, with potentials of −48 and −80 mV vs. Hg/HgO reported at 100 mA cm^{-2} with oxygen and air, respectively and −190 mV at 1A cm^{-2} with O_2 [28]. An air cathode consisting of 10% CoTMPP on activated carbon (14 mg cm^{-2}) gave a performance in 7 M KOH and 25 °C at 100 mA cm^{-2} of −120 mV vs. Hg/HgO with a minimal potential loss of 20 μV/h after 4600 h of operation for electrodes treated at 810 °C (Hg/HgO) [29].

Fe-TMPP was tested in an anion exchange membrane fuel cell (AEM) giving an OCP similar to that of platinum of ca. 1.1 V (1 $mg_{catalyst}$ cm^{-2}) and a power density of 30 mW cm^{-2}. However the catalyst was not heat treated and therefore suffered instability in the amine environment used [3].

This current work focused on evaluation Co based commercial catalysts from GPMaterials (France) for cathode materials in liquid alkaline electrolyte and in alkaline anion exchange membrane fuel cells.

2. Experimental

2.1. Electrochemical measurements

The electrochemical studies were carried out using a standard three-electrode cell and an Autolab bipotentiostat (PGSTAT 302). The rotating ring disc electrode was from Pine instrument (AFMSRC 2092). The rotating ring disc electrode was a glassy carbon disk with a surface area of 0.2475 cm^2 and ring was platinum with a surface area of 0.1866 cm^2 with a collection efficiency of 37%. A platinum wire (surface area 3.6 cm^2) was used as a counter and mercury/mercury oxide (Hg/HgO, radiometer) electrode in 1 M KOH solution (+0.14 V vs. SHE) was used as a reference electrode. All the potentials reported in this study are referred to the standard hydrogen electrode (SHE).

The Co-based/C catalyst (ca. ∼4 wt%) with a loading of 2 $mg_{catalyst}$ cm^{-2} (i.e. 80 μg cm^{-2} cobalt complex) on a glassy carbon electrode (GCE) was prepared by the following procedure. The catalyst ink was prepared by mixing the required quantity of Co-based catalyst (GPMaterials, Aix les Bains, France) catalyst in 0.5% Nafion® solution. The mixture was sonicated for 30 min in an ultrasonication bath. 5 μl of the catalyst slurry was carefully dropped onto the GCE surface and allowed to dry at room temperature for 15 min to obtain a uniform catalyst film. All electrochemical experiments were carried out at room temperature and ambient pressure employing 1 M KOH as the electrolyte solution.

2.2. Membrane preparation

The membranes were produced by the mutual radiation grafting technique similar to those described in previous papers [3,7,30].

The aminated poly (LDPE-*co*-VBC) membranes were produced by the mutual radiation grafting technique as described in previous papers [3,7,30]. Pieces of the required polymer were initially weighed and then interleaved with a non-woven material and rolled up into a "Swiss roll" configuration. The roll was placed in a glass grafting tube and filled with monomer solution until the complete roll was saturated and covered. The oxygen in the vessel was then removed by purging with nitrogen. The irradiation was carried out at 23 ± 1 °C using a Cobalt 60 gamma radiation source for a pre-determined time at a known dose rate. Once grafted, the films were washed in toluene to remove any homopolymer, prior to drying to constant weight in an oven at 70 °C. The degree of grafting (DOG) of the membrane, which represents the proportion of the grafted polymer in the membrane was calculated using the following formula:

$$\mathrm{DOG\%} = \frac{W_g - W_o}{W_g} \times 100 \quad (1)$$

where W_g is the weight of grafted copolymer and W_o is the weight of polymer film before grafting. Therefore, a polymer with a DOG = 32%, consists of 32% of the grafted monomer and 68% original polymer.

In order to impart functionality on the grafted copolymer, the dry grafted copolymer was reacted in a solution of 50% aqueous trimethylamine (TMA) for 4 h at ambient temperature, after which the films were washed to neutrality using demineralised water.

Membrane used in this study exhibited a DOG of 32% starting with 50 μm low density polyethylene (LDPE). The final membrane thickness obtained in OH^- form and fully hydrated conditions were 90 μm.

The membrane conductivity was measured using the four point probe technique, when fully hydrated, with values in the temperature range of 20–60 °C from 0.04 to 0.076 S cm^{-1} [31]. At 80 °C, the conductivity reached 0.083 S cm^{-1}.

2.3. Fuel cell testing

Fuel cell electrodes were made from catalyst inks to which PVBC was added to facilitate ionic conductivity. The catalyst ink was prepared by sonicating the catalyst 30% Pt/C (ETEK, USA) or Co-based/C (GP2-GPM or GP4-GPM) with 30 wt% PVBC in acetone. The catalysts carbon support was Vulcan XC-72 for Pt and GP2-GPM, and graphite for GP4-GPM. The ink was then airbrushed on a gas diffusion electrode, (non-woven carbon cloth) incorporated with wet proofed micro porous layer (Freudenberg FFCCT, Germany) referred to as GDL. The catalyst loading were 0.5 mg_{Pt} cm^{-2} (1.66 $mg_{catalyst}$ cm^{-2}) and Co-based/C (3 $mg_{catalyst}$ cm^{-2}).

The electrodes were then immersed in N,N,N′,N′-tetramethyl-1,6-hexanediamine (TMHDA, Acros) for 3 h and washed several times with de-ionised (DI) water. The resulting electrode and the membrane were converted to OH^- conducting group by immersing them in 1.0 M KOH for 3 h and changing the solution every 30 min.

For the experimental single cell, titanium was used with 1 cm^2 serpentine flow fields surrounded by O-ring seal. The temperature of the cell was controlled by thermostatically controlled cartridge heaters inserted into the cell body. The anode gas was passed into a home-made humidifier at temperature of 10 °C higher than the cell operating temperature prior to entering the cell, this provided humidification conditions close to 100% RH. The flow rates were controlled manually by means of appropriate flow meters for each gas (Platon (RM&C), U.K.). The cell was tested under ambient pressure unless otherwise specified and all gases used were CO_2 free grade.

Polarisation curves were recorded using a cathodic sweep at a scan rate of 5 mV s^{-1} by employing Autolab PGSTAT 30 (Eco Chemie, The Netherlands). The electrodes were subject to several cycles

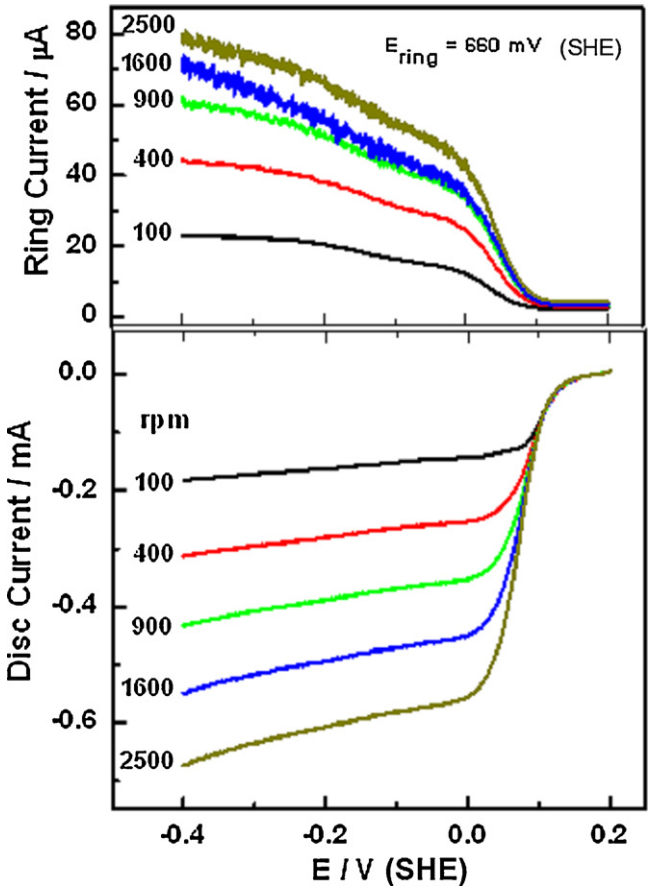

Fig. 1. Rotating ring-disc electrode response recorded at 5 mV s^{-1} scan rate for Co-based/C (GP2) in O_2-saturated 1 M KOH solution at different rotation rates as indicated in the figure.

until a steady performance was reached. Previous tests confirmed that this was slow enough to approximate to steady state operation [3]. The relative humidity was obtained from an intrinsically safe humidity sensor (Vaisala HUMICAP®, Finland).

3. Results and discussion

3.1. ORR studies on Co-based/C catalyst surface by RRDE technique

To evaluate the electrocatalytic activity of the ORR on Co-based catalysts, RRDE tests were carried out. Fig. 1 shows the dependence of the RRDE measurements for Co-based/C thin film electrode on the rotation rate. The ORR started at 120 mV and gradually passed through a mixed control between 90 mV and −40 mV to complete mass-transfer control when the potential reached less than −40 mV. The expected increase in the diffusion limited current in the disk measurement was observed as a function of rotation speed. Similarly the measured ring current at 0.66 V, i.e. oxidation of hydrogen peroxide produced during ORR, also increased with rotation rate as shown in Fig. 1.

The Koutecky–Levich plots at different potentials showed a linear dependence at all potentials (Fig. 2). However the plots were not parallel at different potentials studied. An estimate of number of electrons in the ORR can be calculated from the Koutecky–Levich equation:

$$\frac{1}{i} = \frac{1}{i_k} + \frac{1}{i_d} = \frac{1}{i_k} + \frac{1}{B\omega^{1/2}} \quad (2)$$

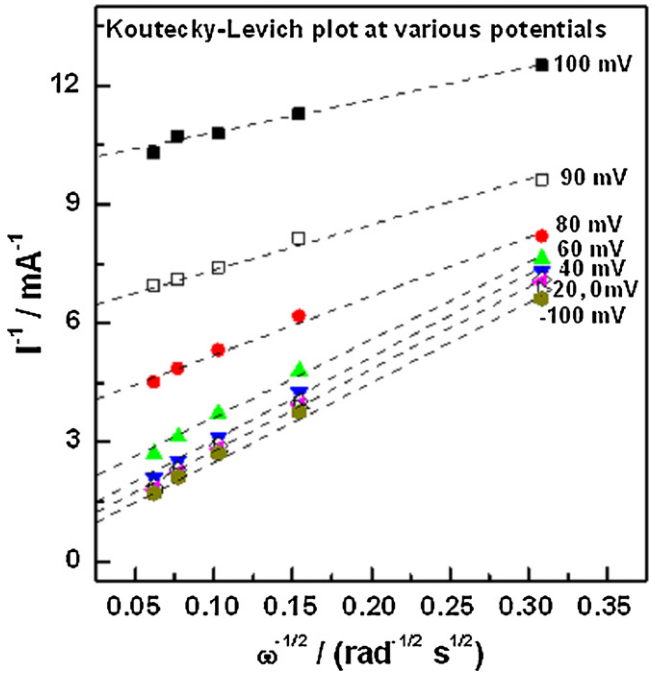

Fig. 2. Koutecky–Levich plots drawn at different potentials (vs. SHE).

where i is the measured current, i_k is the kinetic current, B is a constant, and ω is the rotation rate (rad s^{-1}). The values of the diffusion coefficient of O_2 ($D_{O_2} = 1.93 \times 10^{-5}$ cm^2 s^{-1}), the kinematic viscosity of the solution ($\nu = 1.1 \times 10^{-2}$ cm^2 s^{-1}), and the concentration of dissolved O_2 in solution ($C_{O_2} = 1.2 \times 10^{-3}$ mol L^{-1}) were used to calculate $B = 0.62nFAD_{O_2}{}^{2/3}\nu^{-1/6}C_{O_2}$, where F is the Faraday constant and A is the electrodes geometric area.

The resultant n value from the slope of Koutecky–Levich plot drawn at −0.4 V (limiting current region) was found equals to 2.2, which testifies that the ORR on Co-based catalyst proceeds via a two electron path way rather than a four-electron reduction in agreement with the literature [20–22]. The value also in general agreement with the calculated value of 2.9 obtained from Eq. (3) below, assuming 51% H_2O_2 generation at −0.3 V (Fig. 5):

$$n = \frac{4I_D}{I_D + I_R/N} \quad (3)$$

where I_D is disc current, I_R is ring current and N is the collection efficiency coefficient.

3.2. Comparison of ORR activities on Co-based/C and Pt/C catalyst surfaces

Fig. 3 compares the ORR activity on commercial Co-based/C vs. E-Tek 20% Pt/C under identical experimental conditions in terms of the linear sweep voltammetery (LSV) curves recorded with a rotation rate of 2500 rpm and at a 5 mV s^{-1} scan rate in 1 M KOH solution.

The mass-transfer corrected kinetic current $(i_k)_{\omega\to 0}$ derived at each potential from Koutecky–Levich plot and the geometric surface area of glassy carbon electrode were used to obtain kinetic current density (j_k) and to construct Tafel plots to assess the specific activity (i_s) at differ potentials. The extraction of Tafel slopes was made from the two linear-region of the plot; ca. 100 to −100 mV. Within experimental error the Tafel slope was 120 mV dec^{-1}, as shown in Fig. 4, and in agreement with the reported values in the literature for the same potential range [20,24].

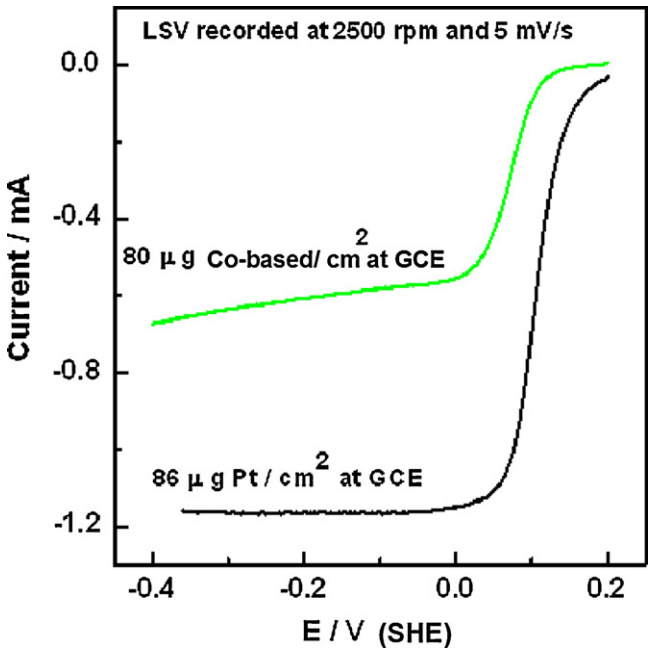

Fig. 3. LSV response recorded at 5 mV s^{-1} scan rate for Co-based/C (GP2) and Pt/C in O_2-saturated 1 M KOH solution at 2500 rpm rotation rate.

It is clear from Fig. 3 that the on-set potential for Co-based catalyst was 120 mV more negative when compared vs. Pt/C catalyst. Moreover, the mass-transfer limiting current region of Pt/C catalyst was almost twice that of the Co-based catalyst. This indicated that the 2 electron transfer process is the most dominant reaction with Co-based catalyst, where peroxide generation is larger than 50% (Fig. 5) at low potentials of −300 mV in comparison to the 4 electron transfer process on Pt (peroxide generation is ca. 5%, Fig. 5).

The relatively small difference in the onset potential between Pt/C and Co-based/C catalysts however suggests the latter may be a promising cheap alternative to platinum in an alkaline environment for ORR.

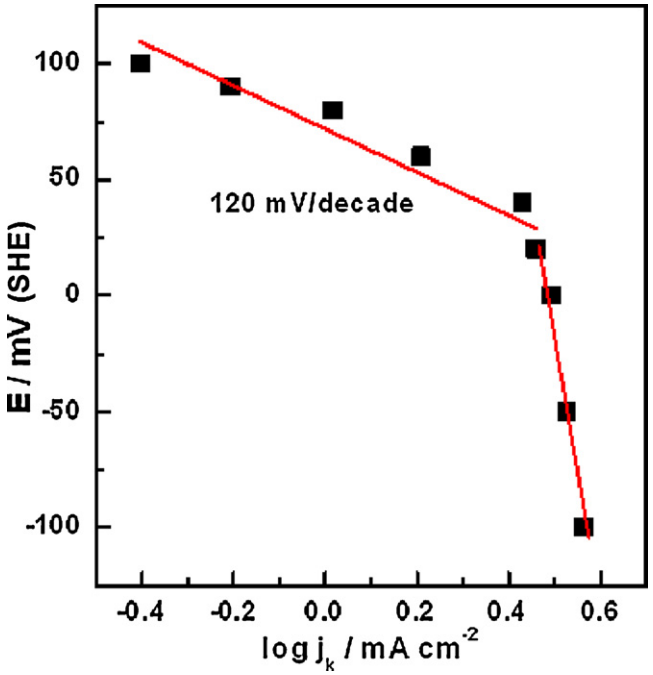

Fig. 4. Mass-transfer corrected Tafel plot for Co-based/C catalyst.

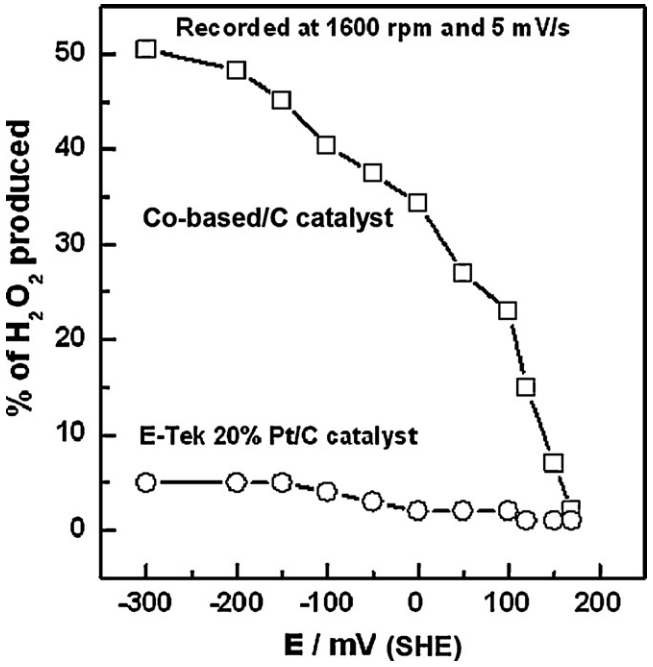

Fig. 5. The H_2O_2 produced (%) during ORR at Co-based/C and Pt/C catalysts surfaces in 1 M KOH solution.

3.3. Estimation of the amount of hydrogen peroxide produced during ORR

The percentages of the current associated with peroxide generation at different potentials were calculated using Eq. (4):

$$H_2O_2\% = \frac{2I_R}{NI_D + I_R} \quad (4)$$

where I_D is the disc current, I_R is ring current and N is the collection efficiency coefficient.

Fig. 5 shows the variation in the amount of H_2O_2 produced by Co-based catalyst with potential during ORR, obtained at a 1600 rpm rotation rate, using 5 mV s^{-1} scan rate in 1 M KOH solution. The amount of hydrogen peroxide produced increased sharply as potentials become more negative. For example, H_2O_2% was 8% at 150 mV (vs. SHE) and increased to ca. 30% at 0 mV. Moreover, the amount of hydrogen peroxide produced at Pt/C surface was 5% even at more negative potentials. The large amount of peroxide generation in Co-based/C catalyst is well documented in the literature [18,22,27] and is not surprising given the high percentage of carbon in the Co-based catalyst with typical cobalt based precursor, i.e. ca. 3 wt%.

3.4. Fuel cell performance

3.4.1. Cell performance of Co-based catalyst

Performance comparison between MEAs utilizing platinum and Co-based (GP2) as cathode catalyst for ORR in AAEM at 20 °C are shown in Fig. 6. Vulcan XC-72 was the carbon support for both catalysts. At 50 mA cm^{-2} the differences in cell potential was only 45 and 67 mV (Table 1) between the stable performance of platinum (higher) and cobalt cathodes with air and oxygen, respectively. Open circuit voltages for Pt cathode were 1.04 and 1 V in comparison to 0.96 and 0.95 V for GP2-GPM for oxygen and air, respectively. This corresponds to potential difference of 80 and 50 mV between the two catalysts under oxygen and air, respectively. The values are lower than the difference measured in liquid KOH earlier, i.e. 120 mV with oxygen. The AAEM (ionomer) environment is different to that of liquid KOH. It has been reported previously [3] that

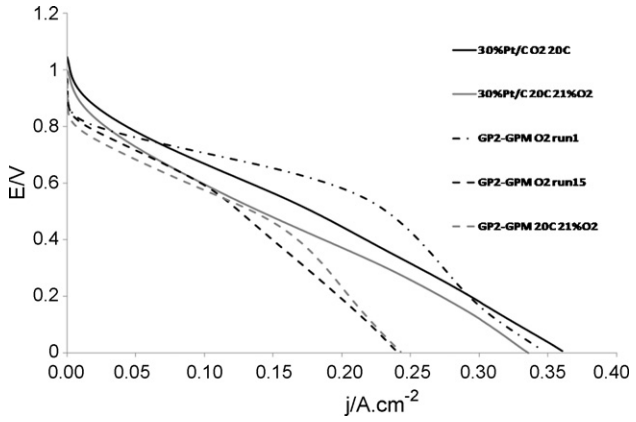

Fig. 6. Performance comparison between MEAs utilizing platinum and Co-based as cathode catalyst for ORR in AAEM at 20 °C with oxygen and air (atm).

Table 1
Cell potentials in mV at 50 mA cm^{-2} at different conditions using 30% Pt/C, GP2 and GP4 at the cathode.

	20 °C	40 °C	60 °C
30% Pt/C air	728	832	827
30% Pt/C air (1 bar)	–	–	867
30% Pt/C O_2	782	870	894
GP2-GPM air	683	699	726
GP2-GPM air (1 bar)	–	–	753
GP2-GPM O_2	715	733	766
GP4-GPM air	658	709	717
GP4-GPM air (1 bar)	–	–	754
GP4-GPM O_2	694	733	758

Fe-TMPP had a special interaction with the quaternized ammonium group in AAEMFC leading to different ORR characteristics than that in liquid KOH. A hysteresis was seen in this work for Co-based catalyst between the first cycle and the subsequent cycles (2nd–30th cycle) where a stable performance was observed. This phenomenon was also observed at 40 °C (Fig. 7) and 60 °C and was also observed regardless of the carbon support used (Fig. 9) and was reproducible when the electrode were left at OCP for 10 min and the cycles restarted. The active first cycle of GP2-GPM exhibited smaller polarisation slopes than that of Pt. Since both MEAs utilized the same membrane and ionomer content, and had similar resistivity (ca. 80 mΩ from FRA), and by ignoring mass transport effect at low current density under O_2 operation, the difference in the polarisation slopes can be attributed to difference in the kinetics of ORR on both catalysts (i.e. Tafel slopes) [32].

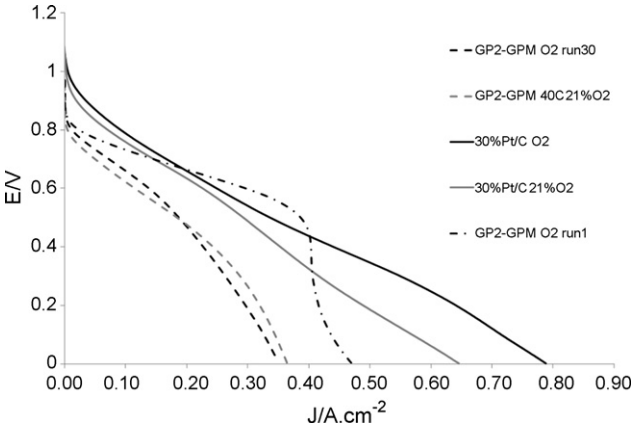

Fig. 7. Performance comparison between MEAs utilizing platinum and Co-based as cathode catalyst for ORR in AAEM at 40 °C with oxygen and air (atm).

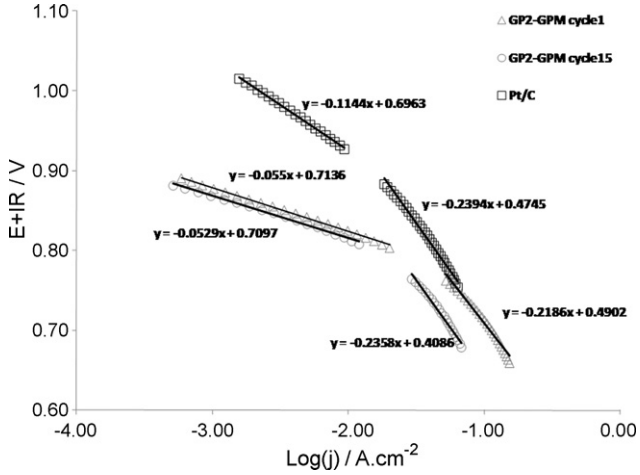

Fig. 8. IR corrected Tafel plots of platinum and Co-based cathodes in AAEM at 20 °C with oxygen (atm).

The difference in the polarization slope can be caused by difference in Tafel slope between the two catalyst. Tafel analysis of IR corrected polarization curves (under oxygen) in the potential range of 1.0–0.7 V (vs. RHE) is shown in Fig. 8. The reported Tafel slope for platinum in liquid 1 M KOH at low current density is ca. 60 mV dec^{-1} and at high current density varied from 120 [33], >200 [34], 260 [35] and in the range of −100 to −300 mV dec^{-1} [36]. In this work, the Tafel slope at the AAEM interface for platinum was ca. 120 mV dec^{-1}, for the low current region, and ca. 240 mV dec^{-1}, for the high current density region. GP2 on the other hand exhibited Tafel slope of ca. 60 mV dec^{-1} in the low current density region and close to 240 mV dec^{-1}, in the high current region. The obtained value in AAEM environment in the low current range of 60 mV dec^{-1} is half that measured in liquid 1 M KOH earlier, which shows the importance of the surrounding fuel cell environment for the ORR kinetics.

No significant difference was observed in the first Tafel slopes of the 1st and 15th cycle of GP2 catalyst. The second Tafel slope was slightly lower in the 1st cycle (219 mV dec^{-1}) than that of the 15th (236 mV dec^{-1}). The difference in the current density (activity) seems to increase with decreased cathode potential. For example, at 850 mV the current density of the 1st cycle was ca. 1.5 times that of the 15th (3.39 and 2.32 mA cm^{-2}), the current density ratio increased to 2 at 700 mV (114 and 58.2 mA cm^{-2}).

In low current density region, up to 10 mA cm^{-2}, GP2 exhibited a Tafel slope of around half that of platinum (60 vs. 120 mV dec^{-1}). At higher current densities, above 10 mA cm^{-2}, the Tafel slope for platinum increased to ca. 240 mV dec^{-1}. On the other hand, the higher Tafel slope for GP2 appeared at higher current densities in the mid range of 10–100 mA cm^{-2}.

While platinum exhibited a higher onset potential and current density (at low over-potentials) than GP2, its higher Tafel slope means there will be a certain potential when the GP2 activity would surpass that of platinum as seen in the GP2 1st cycle at ca. 750 mV. This shows the great attraction of Co-based catalyst for ORR in AAEMFC environment, especially if the performance achieved from the first cycle could be sustained. This behavior is beyond the scope of this article and will be investigated further and reported in future publications.

3.4.2. Carbon support

The effect of the carbon support on the activity of the Co-based catalyst was studied by comparing the performance of two cathodes utilizing Vulcan XC-72 (GP2) and graphite (GP4) as carbon support (Fig. 9).

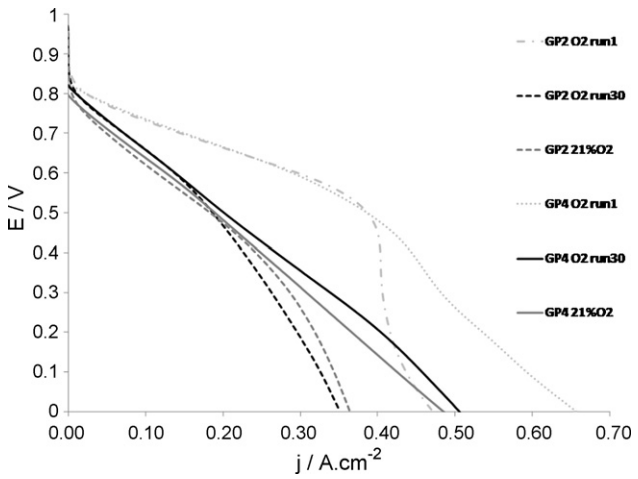

Fig. 9. Performance comparison for Co-based cathode MEAs with Vulcan XC-72 (GP2) and graphite (GP4) as carbon support at 40 °C with oxygen and air (atm).

Catalysts utilizing either support (GP2 and GP4) showed the same behavior regarding the high activity of the first cycle which then fell to a stable performance after a few cycles. Both cathodes showed very similar stable performance (even after 30 cycles) in the kinetic and Ohmic regions. Cathodes utilizing GP4 catalyst, however, exhibited slightly higher limiting current than those utilizing GP2. The difference in the limiting currents can be explained by the difference in density between graphite (2.23 g cm^{-3}) and Vulcan XC-72 (1.7–1.9 g cm^{-3}) [32] at 20 °C, leading to thinner catalyst layer (using the same loading) in the graphite (GP4) case and therefore slightly enhanced mass transport.

The similarity in the activity of GP2 and GP4 suggests that carbon support does not seem to play an important role in the Co-based catalyst activity in AAEMFC.

3.4.3. Power density

Comparison between peak power densities obtained with AAEMFCs utilizing platinum and GP4 as cathode catalyst is shown in Fig. 10. As discussed earlier, while platinum exhibited higher OCPs and higher current densities at potentials down to 0.6 V than GP4, the stable GP4 performance surpassed that of platinum at potentials below 0.6 V due to the smaller GP4 polarization slope.

Power densities of 260, 200 and 145 mW cm^{-2} were achieved with both MEAs under oxygen, air 1 bar (gauge) and air cathode feed (60 °C). While the peak power density for platinum was achieved at a potential of 570 mV (air and air 1 bar), the same peak power density was achieved in GP4 case at a potential of 487 mV (air and air 1 bar). This means that GP4 catalyst achieved the same stable power density as platinum but at a lower efficiency 47.5–40%.

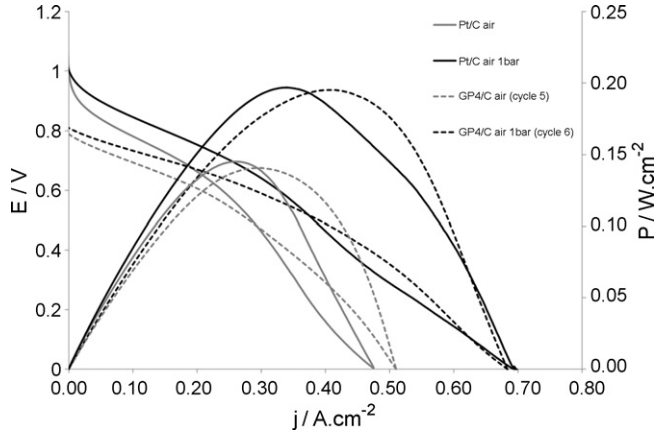

Fig. 10. Peak power density comparison between MEAs utilizing platinum and Co-based as cathode catalyst for ORR in AAEM at 60 °C with air (atm) and air 1 bar (gauge).

The achieved power densities are very promising, some of the highest reported in the literature for non-nobel metal cathodes in alkaline anion exchange membrane fuel cells. Power densities of 15 and 33 mW cm^{-2} are reported for AAEMFCs with Ag/C and Au/C cathodes, respectively, using similar VBC-grafted membrane at 50 °C (ETFE) under oxygen [37].

4. Conclusions

Co based catalysts (GP2 and GP4) were used for the oxygen reduction reaction in both liquid KOH and alkaline anion exchange membrane fuel cells AAEMFCs. In liquid KOH solution the catalysts exhibited good performance with onset potentials 120 mV more negative than platinum and Tafel slopes of ca. 120 mV dec^{-1}. The amount of the generated hydrogen peroxide increased from 5 to 50% as the electrode potential decreased from 175 to −300 mV vs. SHE.

In an AAEMFC environment potential differences between the platinum (more positive) and GP2 of 80 and 50 mV were observed with oxygen and air, respectively. GP2 showed promising performance for ORR, at 50 mA cm^{-2} differences in cell potential between the stable performance of platinum (higher) and cobalt cathodes with air and oxygen, were only 45 and 67 mV respectively.

GP4 catalyst achieved the same stable power density of platinum of 200 and 145 mW cm^{-2} with air 1 bar (gauge) and air cathode feed (60 °C), respectively, although with a lower efficiency of 40% in comparison to platinum 47.5%. This indicates that the Co-based catalyst are promising alternative catalysts to platinum for oxygen reduction in AAEMFCs.

Acknowledgements

The authors acknowledge the support of the EPSRC for funding. The authors also like to thank Dr. J.A. Horsfall and Dr. C. Williams from Department of Materials & Medical Sciences, Cranfield University, U.K., for their generous membranes supply for this study under EPSRC project “Alkaline Polymer Electrolyte Membrane Fuel Cells (APEMFCs)”.

References

[1] E. Hao Yu, K. Scott, R.W. Reeve, J. Electroanal. Chem. 547 (2003) 17–24.
[2] J.R. Varcoe, R.C.T. Slade, Fuel Cells 5 (2005) 187–200.
[3] M. Mamlouk, X. Wang, K. Scott, J.A. Horsfall, C. Williams, J. Power Energy 225 (2011), doi:10.1177/2041296710394264.
[4] E.H. Yu, K. Scott, Electrochem. Commun. 6 (2004) 361–365.
[5] R.C.T. Slade, J.R. Varcoe, Solid State Ionics 176 (2005) 585–597.
[6] J.R. Varcoe, R.C.T. Slade, Electrochem. Commun. 8 (2006) 839–843.
[7] H. Cheng, K. Scott, K.V. Lovell, J.A. Horsfall, S.C. Waring, J. Membr. Sci. 288 (2007) 168–174.
[8] L. Li, Y. Wang, J. Membr. Sci. 262 (2005) 1–4.
[9] J. Pan, S. Lu, Y. Li, A. Huang, L. Zhuang, J. Lu, Adv. Funct. Mater. 20 (2010) 312–319.
[10] J. Wang, S. Li, S. Zhang, Macromolecules 43 (2010) 3890–3896.
[11] Y. Wu, C. Wu, J.R. Varcoe, S.D. Poynton, T. Xu, Y. Fu, J. Power Sources 195 (2010) 3069–3076.
[12] J. Fang, P.K. Shen, J. Membr. Sci. 285 (2006) 317–322.
[13] M.R. Hibbs, C.H. Fujimoto, C.J. Cornelius, Macromolecules 42 (2009) 8316–8321.
[14] E.E. Switzer, T.S. Olson, A.K. Datye, P. Atanassov, M.R. Hibbs, C. Fujimoto, C.J. Cornelius, Electrochim. Acta 55 (2010) 3404–3408.
[15] Y. Luo, J. Guo, C. Wang, D. Chu, J. Power Sources 195 (2010) 3765–3771.
[16] R. Jasinski, Nature 201 (1964) 1212–1213.
[17] K.I. Ozoemena, S.A. Mamuru, T. Fukuda, N. Kobayashi, T. Nyokong, Electrochem. Commun. 11 (2009) 1221–1225.
[18] R. Yang, K. Stevens, A. Bonakdarpour, J.R. Dahn, J. Electrochem. Soc. 154 (2007).
[19] X. Li, G. Liu, B.N. Popov, J. Power Sources 195 (2010) 6373–6378.
[20] L. Mao, K. Arihara, T. Sotomura, T. Ohsaka, Electrochim. Acta 49 (2004) 2515–2521.
[21] H. Qin, S. Lao, Z. Liu, J. Zhu, Z. Li, Int. J. Hydrogen Energ. 35 (2010) 1872–1878.

[22] T.S. Olson, S. Pylypenko, P. Atanassov, A. Koichiro, Y. Koji, T. Hirohisa, J. Phys. Chem. C 114 (2010) 5049–5059.
[23] P. Gouerec, A. Bilou, O. Contamin, G. Scarbeck, M. Savy, J.M. Barbe, R. Guilard, J. Electroanal. Chem. 398 (1995) 67–75.
[24] R. Chen, H. Li, D. Chu, G. Wang, J. Phys. Chem. C 113 (2009) 20689–20697.
[25] V. Bambagioni, C. Bianchini, J. Filippi, A. Lavacchi, W. Oberhauser, A. Marchionni, S. Moneti, F. Vizza, R. Psaro, V. Dal Santo, A. Gallo, S. Recchia, L. Sordelli, J. Power Sources 196 (2011) 2519–2529.
[26] P. Gouerec, M. Savy, Electrochim. Acta 44 (1999) 2653–2661.
[27] A. Li Zhu, H. Wang, W. Qu, X. Li, Z. Jong, H. Li, J. Power Sources 195 (2010) 5587–5595.
[28] Y. Kiros, S. Schwartz, J. Power Sources 36 (1991) 547–555.
[29] I. Iliev, S. Gamburzev, A. Kaisheva, J. Power Sources 17 (1986) 345–352.
[30] J.A. Horsfall, K.V. Lovell, Eur. Polym. J. 38 (2002) 1671–1682.
[31] M. Mamlouk, K. Scott, Int. J. Hydrogen Energ. (2011), doi:10.1016/j.ijhydene.2011.03.074.
[32] M. Mamlouk, K. Scott, Int. J. Hydrogen Energ. 35 (2010) 784–793.
[33] D.B. Sepa, M.V. Vojnovic, L.M. Vracar, A. Damjanovic, Electrochim. Acta 32 (1987) 129–134.
[34] K.L. Hsueh, E.R. Gonzalez, S. Srinivasan, Electrochim. Acta 28 (1983) 691–697.
[35] K. Tammeveski, M. Arulepp, T. Tenno, C. Ferrater, J. Claret, Electrochim. Acta 42 (1997) 2961–2967.
[36] L. Geniès, R. Faure, R. Durand, Electrochim. Acta 44 (1998) 1317–1327.
[37] S.D. Poynton, J.P. Kizewski, R.C.T. Slade, J.R. Varcoe, Solid State Ionics 181 (2010) 219–222.